Pneumatic webbed soft gripper for unstructured grasping

Shibo Cai[1,2], Chun'e Tang[3], Lufeng Pan[1], Guanjun Bao[1,2], Wenyu Bai[1,2], Qinghua Yang[1,2*]

(1. *College of Mechanical Engineering, Zhejiang University of Technology, Hangzhou 310023, China*;
2. *Key Laboratory of Special Purpose Equipment and Advanced Processing Technology, Ministry of Education and Zhejiang Province, Zhejiang University of Technology, Hangzhou 310023, China*;
3. *Instrumentation Technology and Economy Institute, Beijing 100055, China*)

Abstract: Grasping unstructured and fragile objects such as food and fruits is a great challenge for robots. Being naturally different from the traditional rigid robot, soft robotics provide highly promising choices with their intrinsic flexibility and compliance to objects. Inspired by duck foot and octopus tentacle, a pneumatic webbed soft gripper was proposed, which is consisted of four multi-chambered fingers and four webs. Due to its silicone body and soft web structure, the developed soft gripper can naturally adapt, grasp and hold delicate and unstructured objects. Compressed air inflated into the three chambers of the finger actuates the silicone body and performs inflection and extension. The silicone web follows the motion of four fingers, forming a semi-closed grasping configuration. The fingers were fabricated with silicone rubber and constraint spring by casting process. The web was cast around the fingers. The inflecting motion was modeled via the pneumatic principle and geometrical analysis. The dynamic properties of the finger were tested by step and sinusoidal signals. And the grasping performances for different objects, such as egg, strawberry, candy, and knife, were also demonstrated by experiments. The proposed soft gripper performed stably in response to a 0.4 Hz reference sinusoidal signal. The bionic structure greatly improves the stability and reliability of grasping, particularly for unstructured and fragile objects. Moreover, the webs ensure the grasping for multiple objects in one snatch, especially suitable for agricultural products and food processing.
Keywords: soft gripper, biomimetics, grasping, robotic, pneumatic
DOI: 10.25165/j.ijabe.20211404.6388

Citation: Cai S B, Tang C E, Pan L F, Bao G J, Bai W Y, Yang Q H. Pneumatic webbed soft gripper for unstructured grasping. Int J Agric & Biol Eng, 2021; 14(4): 145–151.

1 Introduction

In recent years, soft robotics[1,2] witnesses enormous development and promising application in many fields. As one of the hot topics in this new area, soft gripper has attracted vast interest and been widely investigated. And various forms of soft grippers have been designed and developed. Generally, they are three-fingered or four-fingered grippers. For example, the Multi-Choice Gripper is a multi-functional three-fingered gripper developed by Festo company[3], which can be freely switched between the two gaits of parallel gripping and center gripping. Before that, Suzumori et al.[4] developed a four-fingered pneumatic flexible gripper, which is able to perform relatively complicated operations, such as turning screws, grasping coins, and operating beaker. Also, the Utah/MIT hand[5] is a four-fingered flexible gripper, which can do precise grasping. In terms of grasping performance, the above-mentioned soft grippers are generally suitable for only one single object. In the case of jumble targets, such as the collection of parts and a bunch of candies, it is quite challenging for current grippers to perform the unstructured multibody grasping. Moreover, due to the natural defects of insufficient rigidity and poor stability of soft materials[6], soft grippers can hardly grasp objects with complex shapes, small volumes, and heavy weights. It will not be difficult to imagine that the tiny objects might be hard to be clamped and tend to slip off the fingers.

Many of the developed soft grippers took inspiration from soft-bodied invertebrate animals, such as octopuses and earthworms[7,8]. Animals exploit soft structures to move effectively in complex natural environments. These capabilities have inspired scientists and engineers in robotics field to incorporate soft technologies into their research and designs, especially focusing on imitating the structure, actuation, and abilities of the soft animals.

This work tried to develop a soft gripper that can hold multiple diminutive objects in one snatch and improve the stability and reliability of grasping. The study proposed a four-finger webbed soft gripper and focused on the design, fabrication, and control. The design inspiration came from the structure of the flippers of ducks, i.e., adding webs to the traditional soft fingers to wrap the objects when grasping them. The webbed soft gripper can effectively prevent the gripped objects from falling off from the gaps between the fingers, and reduce the precision requirements of the capture operation, which greatly improves the success rate and reliability of grasping.

2 Materials and methods

2.1 Materials

The material for soft robots is mostly determined to be silicone

Received date: 2020-12-30 **Accepted date:** 2021-06-08
Biographies: Shibo Cai, PhD, Associate Professor, research interest: soft robotics, Email: ccc@zjut.edu.cn; **Chun'e Tang**, MS, Assistant Engineer, research interest: electromechanical system control, Email: tangchune@instrnet.com; **Lufeng Pan**, MS, research interest: soft robotics, Email: 342526538@qq.com; **Guanjun Bao**, PhD, Professor, research interest: soft robotics, robot dexterous hand, Email: gjbao@zjut.edu.cn; **Wenyu Bai**, PhD, Assistant Professor, research interest: electromechanical system drive, Email: bauyo@zjut.edu.cn.
***Corresponding author: Qinghua Yang**, PhD, Professor, research interest: agricultural robot. College of Mechanical Engineering, Zhejiang University of Technology, Hangzhou 310023, China. Tel: +86-571-85290259, Email: robot@zjut.edu.cn.

or rubber[9,10], since these materials are easily accessible, relatively inexpensive, non-toxic, and can be easily shaped[11]. The silicone with Shore A hardness of 100 was used, which ensures the relatively high air pressure endurance inside the soft fingers required to grasp and support the load. While for the web around the fingers, another silicone material Ecoflex 00-50 was chosen. Ecoflex[12] is a kind of translucent, soft elastomer that is stretchable under quite low stress and provides the capability of adapting and wrapping.

In order to obtain the elastic modulus of the material, the tensile test of the silicone samples[13] was performed with a tensile testing machine. Figure 1 shows the silicone samples with a width of 5.00 mm, a thickness of 1.00 mm, and an effective length of 20.00 mm.

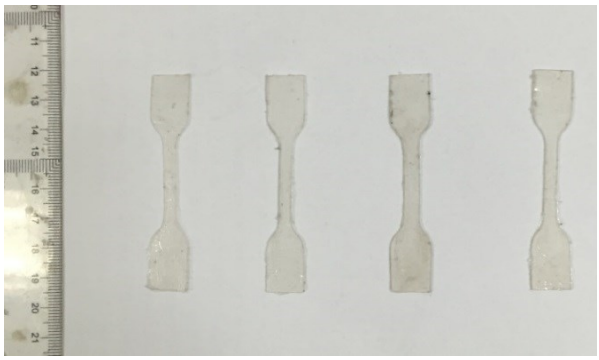

Figure 1 Silicone samples for tensile test

The test results were shown in Figure 2. It can be clearly seen that the stress-strain curves of the five tests showed almost the same trend in the elastic strain stage, and the fracture finally occurred at elongation rates over 1000%. The stress-strain curves are almost linear. So, the elastic modulus E can be obtained by averaging the experimental data of the five samples, which is 0.995 MPa.

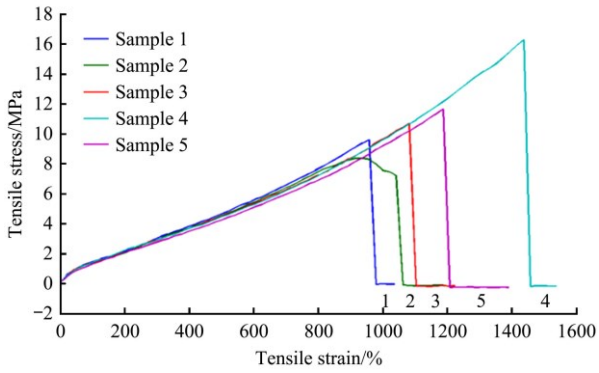

Figure 2 Stress-strain curve of the tensile test

2.2 Actuation

Conventional rigid robots are mainly actuated by motors and relatively complicated mechanical structures which provide rotational and linear motion, while soft robots employ new driving manners, including variable length tendons, fluidic actuation, and electro-active polymer, which can achieve multi-degree of freedom and continuum deformation. As one of the main forms of fluidic actuation, pneumatic actuation[14] employing compressed air as working media possesses many advantages, such as low viscosity, low mass, high availability[15], no pollution[16], and low cost[17]. In this study, a highly flexible actuator with embedded air chambers was developed. As these chambers are inflated with pressurized air, the actuator can perform inflection in any direction. This body morphing allows the operation of grasping.

2.3 Mechanical design

Inspired by the flippers of duck, the webbed structure was designed for the proposed soft gripper. As shown in Figure 3a, the webbed soft gripper consists of four multi-chambered fingers and four webs. The pneumatic fingers are the highly flexible actuators that perform the gripping operation, while the webs will passively follow the motions of the fingers. This synchronous webbed structure greatly increases the contact area between the gripper and objects during grasping, thereby improving the stability and reliability of the operation.

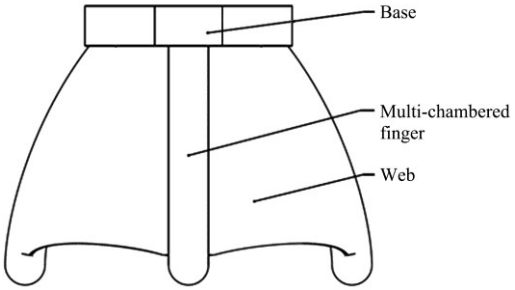

a. Overall structure of the gripper

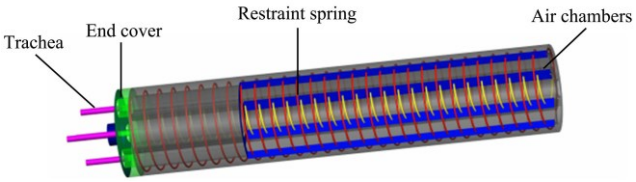

b. Structure of the multi-chambered finger

Figure 3 Structure of pneumatic webbed soft gripper

Imitating the physiological structure of octopus brachiopods[18,19], a three-chamber soft finger as shown in Figure 3b was designed. By controlling the air pressures inside the three air chambers, the finger can bend in any direction.

When the air chambers were inflated, it can be seen that the air chamber will expand rapidly in all directions, due to the intrinsic extensibility of silicone. However, the excessive bulging effect is not beneficial for the grasping operation. In order to control the bending and elongation of the fingers, the longitudinal motion is expected, while the radial expansion has to be eliminated. Furthermore, the limitation of the radial expansion will also in turn enhance the axial elongation.

In order to eliminate the radial expansion of the air chamber, many researchers chose to externally envelop the fiber membranes[20,21] or fiber lines[22,23]. The process of installing the external reinforcement was relatively simple, while the coupling and integration between the flexible material and the external reinforcing material can hardly reach the performance that the internal embedded reinforcement can achieve. Therefore, a spring was internally embedded in the flexible materials so that it can effectively suppress the radial expansion of the fingers, as shown in Figure 3b.

The thickness of the web was set as 2 mm. Using Ecoflex 00-50 can ensure the flexibility to generate the desired deformation, and also maintain a certain degree of rigidity to support the stability of grasping.

2.4 Fabrication

Mold casting is widely used to manufacture soft robots with silicones and other elastomers[24,25]. The molds were designed by computer-aided design and 3D printing with resins[26]. According to the structure shown in Figure 3, four molds are designed for the basal body of fingers (shown in Figure 4a), the outer layer of

fingers, the web between two fingers, and the end cover of the finger for sealing the air chambers, respectively.

The procedure of the fabrication is described as follows:

1) The mold with silicon is used to produce the basal finger body, shown in Figure 4c. The silicon cures for 4 h at room temperature or 15 min at 60°C. (It should be noted that without vacuum operation, curing rapidly at a high temperature will create many bubbles in the finger body, which will badly reduce the quality of the products.) The outer groove of the basal finger body is used to ensure the spring is evenly bound around the finger.

2) Bound spring on the basal finger body is shown in Figure 4d.

3) Secondary mold is to envelop the spring and creates the web connecting two fingers, shown in Figure 4g.

4) The independent webs are pasted on the fingers and the air chambers are sealed by the end cover molded with silicon.

5) The soft gripper was mounted on the base.

The manufactured pneumatic webbed soft gripper is shown in Figure 5.

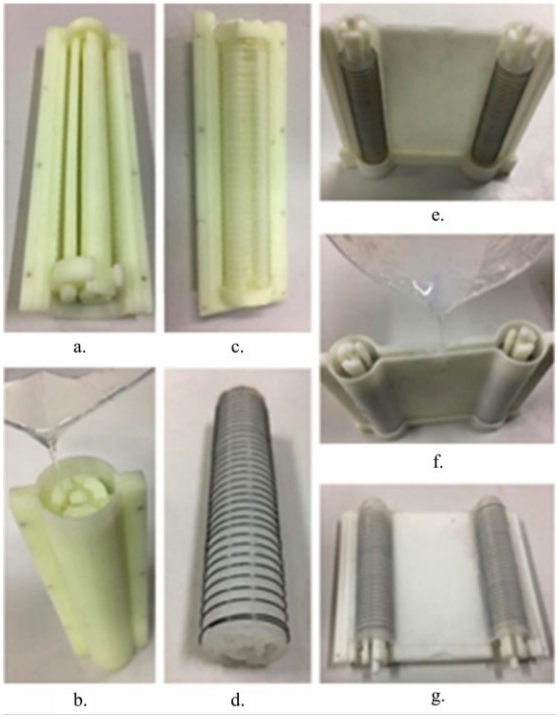

Note: a. Mold for the basal body of fingers was 3D printed and assembled; b. Liquid silicone was poured into the mold; c. First step of molding to obtain the basal finger body; d. Binding the spring on the basal finger body; e. Installing the finger bodies in the mold for the second molding; f. Liquid silicone was poured into the mold; g. Molding to envelop the spring and form the web connecting two fingers.

Figure 4 Fabrication steps of the gripper

Figure 5 Assembled webbed soft gripper

2.5 Actuating model of the soft finger

Figure 6 shows the cross-section of the proposed soft finger, where r_0 is the outer wall radius, r_1 and r_2 are the outer and inner radii of the actuating air chamber, respectively, r_3 is the radius of the stiffness adjusting air chamber, r_{t1} and r_{t2} are the average radii of the inner and outer spring, respectively, and α is the central angle of the actuating air chamber.

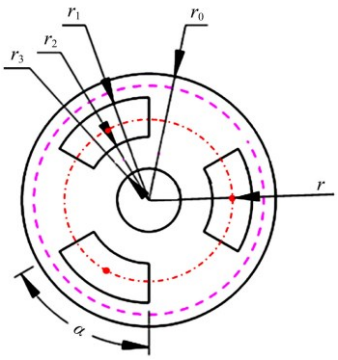

Figure 6 Cross section of the soft finger

The four air chambers can be represented by four springs, which were located at the centroid of the air chambers. Because the three actuating air chambers are equally distributed, the positions of springs are on the same circumferential radius r. According to the geometric relationship in Figure 6, the expression of r can be stated as Equation (1):

$$r = \frac{2\sin\frac{\alpha}{2}(r_1^2 + r_2^2) + r_1^2 - r_2^2}{(r_1 + r_2)\alpha + 2(r_1 - r_2)} \tag{1}$$

A micro-segment of the soft finger was extracted and shown in Figure 7. The line of a-a' in the transverse plane is the neutral axis, and b-b' is the bending axis.

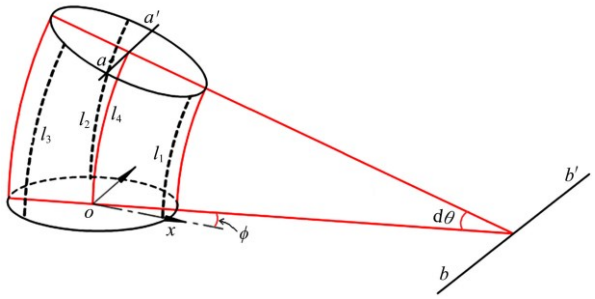

Note: Red lines indicate the cross section.

Figure 7 A micro-segment of the soft finger

According to the geometric relationship in Figure 7, the length of spring models l_1, l_2, l_3, and l_4 can be written as Equations (2)-(5):

$$l_1 = \theta(R_0 - r\cos(-\phi)) \tag{2}$$

$$l_2 = \theta[R_0 - r\cos(\frac{2\pi}{3} - \phi)] \tag{3}$$

$$l_3 = \theta[R_0 - r\cos(\frac{4\pi}{3} - \phi)] \tag{4}$$

$$l_4 = \theta \cdot R_0 \tag{5}$$

where, l_1, l_2, l_3, and l_4 are the lengths of spring models, respectively, mm; R_0 is the radius of curvature of the central axis, mm; ϕ is the yaw angle, rad; θ is the differential angle of the micro-segment, rad.

Then, ϕ, θ and R_0 can be represented with respect to l_1, l_2, and l_3, shown in Equations (6)-(8):

$$\phi = \tan^{-1}\frac{\sqrt{3}(l_3 - l_2)}{l_2 + l_3 - 2l_1} \tag{6}$$

$$\theta = \frac{\sqrt{2[(l_1-l_2)^2+(l_2-l_3)^2+(l_3-l_1)^2]}}{3r} \tag{7}$$

$$R_0 = \frac{(l_1+l_2+l_3)r}{\sqrt{2[(l_1-l_2)^2+(l_2-l_3)^2+(l_3-l_1)^2]}} \tag{8}$$

The elongation of the soft finger is generated by pressurized air and external moment simultaneously, while these two actuating factors are uncoupled. Therefore, the length increment $\Delta(l_i)$ can be represented by Equation (9):

$$\Delta(l_i) = \Delta(l_{ip}) + \Delta(l_{ie}) \tag{9}$$

where, $\Delta(l_{ip})$ is the elongation of the air chamber caused by pressurized air, mm; $\Delta(l_{ie})$ is the elongation of the air chamber caused by external moment, mm.

When only air pressure ΔP_i was applied, the relationship between $\Delta(l_{ip})$ and ΔP_i can be stated as Equation (10):

$$\Delta P_i = \Delta(l_{ip}) \times k \tag{10}$$

where, k is the constant coefficient; ΔP_i is the air pressure inside the chamber, MPa.

When only the external moment M_e was applied, the axial length of the central axis will not elongate and the geometric relationship can be stated as Equations (11)-(13):

$$\Delta(l_{1e}) = r\cos\phi\frac{M_e\Delta L_0}{EI_{a-a'}} \tag{11}$$

$$\Delta(l_{2e}) = r\cos(\frac{2\pi}{3}-\phi)\frac{M_e\Delta L_0}{EI_{a-a'}} \tag{12}$$

$$\Delta(l_{3e}) = r\cos(\frac{4\pi}{3}-\phi)\frac{M_e\Delta L_0}{EI_{a-a'}} \tag{13}$$

where, $I_{a-a'}$ is the moment of inertia transverse to the neutral axis; M_e is the external moment, N·m; E is the Young modulus, MPa; L_0 is the initial length of the finger segment, mm; ΔL_0 is the elongated length of the finger segment, mm.

The scale factor k_M was defined as Equation (14):

$$k_M = \frac{EI_{a-a'}}{r\Delta L_0} \tag{14}$$

According to the independence of the actions of the air pressure and the external moment, the relationship between Δl_i, ΔP_i and M_e can be stated as Equation (15):

$$\begin{aligned}\Delta l_i &= \Delta L_0 + \Delta(l_i) = \Delta L_0 + \Delta(l_{ip}) + \Delta(l_{ie}) \\ &= \Delta L_0 + \frac{\Delta P_i}{k} + \frac{M_e\cos X}{k_M}\end{aligned} \tag{15}$$

where, X represents the position angle of the chamber, $X=\phi$, $(2\pi/3-\phi)$ or $(4\pi/3-\phi)$.

Substituting Equation (15) into Equations (6)-(8), the geometrical parameters of the differential cross section can be obtained as Equations (16)-(18):

$$\phi_i = \tan^{-1}\frac{\sqrt{3}[(\Delta P_3-\Delta P_2)k_M + M_e k(\cos(\frac{4\pi}{3}-\phi)-\cos(\frac{2\pi}{3}-\phi))]}{(\Delta P_3+\Delta P_2-\Delta P_1)k_M + M_e k(\cos(\frac{4\pi}{3}-\phi)+\cos(\frac{2\pi}{3}-\phi)-2\cos\phi)} \tag{16}$$

$$\theta_i = \frac{\sqrt{\begin{aligned}&2[(\Delta P_1-\Delta P_2)k_M + M_e k(\cos\phi-\cos(\frac{2\pi}{3}-\phi))]^2 + \\ &2[(\Delta P_2-\Delta P_3)k_M + M_e k(\cos(\frac{2\pi}{3}-\phi)-\cos(\frac{4\pi}{3}-\phi))]^2 + \\ &2[(\Delta P_3-\Delta P_1)k_M + M_e k(\cos(\frac{4\pi}{3}-\phi)-\cos\phi)]^2\end{aligned}}}{3kk_M r} \tag{17}$$

$$R_{0i} = \frac{[3kk_M\Delta L_0 + k_M(\Delta P_1+\Delta P_2+\Delta P_3)]r}{\sqrt{\begin{aligned}&2[(\Delta P_1-\Delta P_2)k_M + M_e k(\cos\phi-\cos(\frac{2\pi}{3}-\phi))]^2 + \\ &2[(\Delta P_2-\Delta P_3)k_M + M_e k(\cos(\frac{2\pi}{3}-\phi)-\cos(\frac{4\pi}{3}-\phi))]^2 + \\ &2[(\Delta P_3-\Delta P_1)k_M + M_e k(\cos(\frac{4\pi}{3}-\phi)-\cos\phi)]^2\end{aligned}}} \tag{18}$$

where, ϕ_i, θ_i and R_{0i} represent the yaw angle (rad), the bending angle (rad), and the radius of the bent finger (mm), respectively. i=1, 2, 3.

The position and orientation of the soft finger can be described by the above three variables.

3 Experiments

As shown in Figure 8, the scheme of the experimental setup[27] generally includes two sub-systems: control circuit and pneumatic loop.

The NI industrial computer with LabView program was used for signal generating to control the electrical proportional valve, via a shielded junction box. Since the electrical proportional valves need a 24 V power supply and a reference voltage for the input voltage signal, a 24-channel wiring board was added to simplify the circuit. The Industrial Personnel Computer (IPC) is NI PXI-1042Q with eight expansion slots and the controller is NI PXI-8105 based on the Intel Core Duo processor T2500. The NI PXI-6704 was chosen as the analog output card. This module can provide 16-channel voltage output in the range of −10-10 V, 16-channel direct current output in the range of 0-10 mA and 8-channel digital I/O. The shielded junction box is NI SCB-68A which is a plug-in DAQ (Data Acquisition) device with a 68-pin connection port.

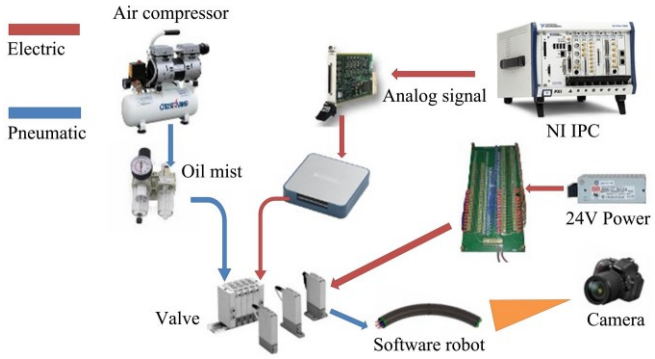

Figure 8 Schematic diagram of the experimental setup

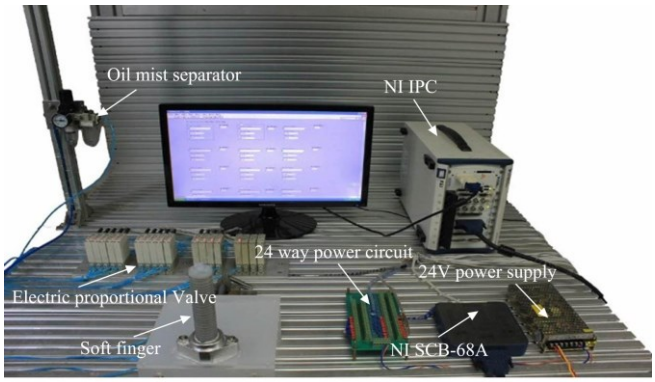

Figure 9 Experimental platform

Air compressor is adopted as the air source. The required pressurized air for the soft gripper comes through an oil mist separator and is regulated by the electrical proportional valve

according to the voltage signal from the electronic control loop. The electrical proportional valve is SMC ITV0050-3BS, whose input control signal ranges from 0 V to 5 V, output pressure ranges from 0.001 MPa to 0.9 MPa with linearity of ±1%.

Based on the experimental scheme, the experimental bed was built, as shown in Figure 9.

3.1 Motion performance of the finger

The finger was mounted on the testbed vertically upwards. Theoretically, when the air pressures in the three chambers are not equal, the finger will bend towards the lower pressure side. The specific bending situation is determined by the coupling pattern of the pressures in the three actuating air chambers. In order to demonstrate the bending performance of the finger more intuitively, there is just inflated one single actuating air chamber, as shown in Figure 10. The air pressures were applied to the actuating air chamber with an increment of 18 kPa to the maximum of 108 kPa. The air pressure and bending angle curve are shown in Figure 11.

As the pressure increases, the bending angle of the finger also rises correspondingly. Before 54 kPa, the experimental data is basically consistent with the theoretical curve. However, the experimental curve goes beyond the model simulation after 54 kPa, which might be caused by the nonlinearity of the elastic action and changing of the silicone body thickness. And due to the inhomogeneity of the material, there are slight differences between the three air chambers. Moreover, the weak stiffness of the finger results in the non-ignorable impact of the gravity during the finger's bending process, which aggravates the nonlinearity of the bending motion, especially when the bending angle getting big and performing high gravity bending moment.

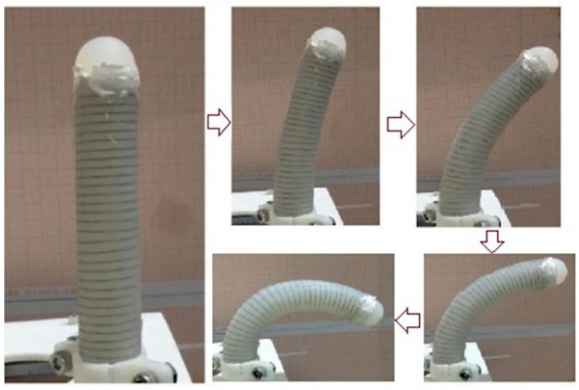

a. Initial state b. Bending process

Figure 10 Bending test of the finger

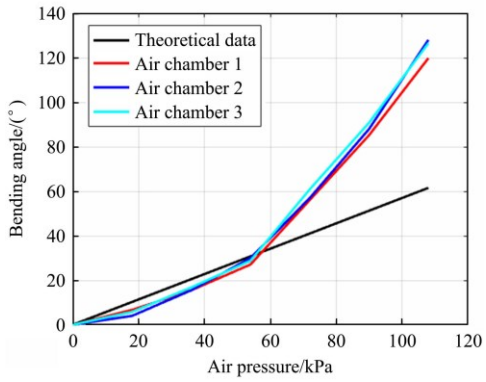

Figure 11 Relationship between air pressure and bending angle of the finger

To demonstrate the dynamic performance of the soft finger, the angular position tracking experiments were executed. The bending angles tracking the reference trajectory were recorded by a six-axis gyroscope (MPU6050)[28,29]. Figure 12 shows the angular response with respect to sinusoidal with the frequency of 0.2 Hz and 0.4 Hz, respectively.

In Figure 12, there are obvious fluctuations of the finger bending angle when it returned to the initial position. This happened because of the influence of the attached measuring unit, which added the concentrated gravity on the fingertip and made the finger difficult to maintain balance at the relative zero-pressure state. Since the stiffness of the finger increases as the air pressure increases, the shaking would be resisted when the finger started to bend under high air pressure. Therefore, the shaking phenomenon only existed at the initial position, when the air pressure in the chamber was close to atmospheric pressure and the rigidity of the finger was minimal. For precise position practice, compensation methods[30] are encouraged to be employed for the controller of the soft gripper.

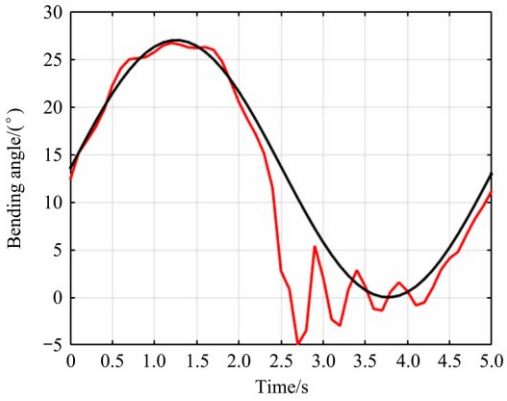

a. Angular response to sinusoidal with frequency of 0.2 Hz

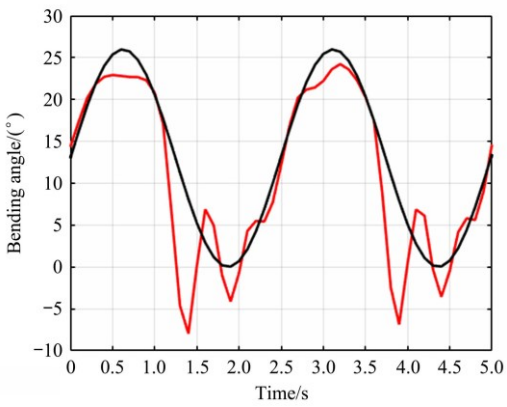

b. Angular response to sinusoidal with frequency of 0.4 Hz

Figure 12 Tracking performance of sinusoidal with different frequencies

Generally, the tracking performance of the assigned trajectory of 0.2 Hz is better than that of 0.4 Hz, while the vibration of the former is server than that of the latter. This is because it takes a certain time to stabilize the air pressure to the predetermined value. Thus, the response characteristic of the finger deteriorates as the frequency increases. It is particularly noticeable that at 0.4 Hz, the finger cannot reach the theoretical bending value at the maximum pressure. And due to the fast inflation that increased the rigidity of the finger timely, the vibration at the initial position can be smoothed more quickly at 0.4 Hz.

Figure 13 shows a dynamic response to the square wave signal. Similarly, the range of air pressure here was set as 0-54 kPa and the corresponding bending angle was 0°-84°.

For the rising edge, the rising time t_r is about 1.33 s. The

quite large damping characteristic was caused by the long process of air pressure establishing due to the nature of the pneumatic system, and the hysteresis of the silicone material. As discussed before, due to the gravity and weak rigidity of the finger under zero pressure, it can be seen that the finger did not return to the initial position precisely at the falling edge.

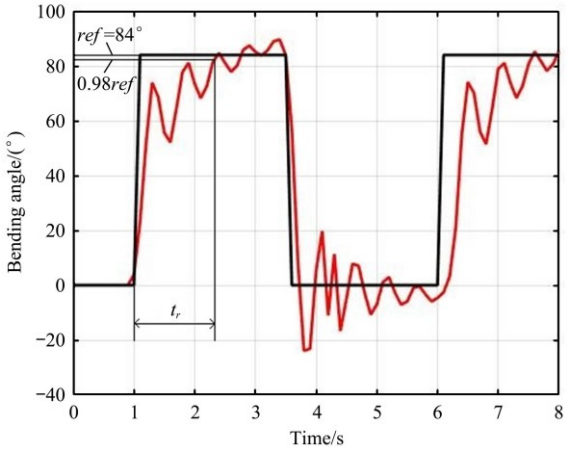

Figure 13 Response of the bending angles for a step signal

3.2 Grasping performance of the webbed soft gripper

When the actuating air chambers at the insides of the fingers were inflated, the fingers opened like a claw as shown in Figure 14a. Due to the severe resistance caused by the elastic force of webs, it was obvious that the bending effect of the finger was reduced in the webbed gripper comparing to that of the independent finger. When the actuating air chambers at the outsides were inflated, the fingers closed together, as shown in Figure 14b.

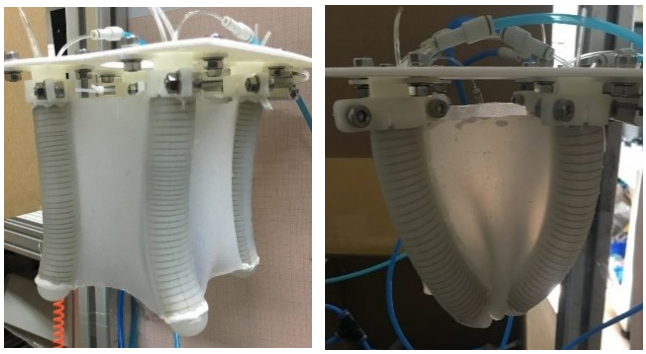

a. Open gesture of the soft gripper (inside actuating air chambers with the pressure of 108 kPa)

b. Closed gesture of the soft gripper (outside actuating air chambers with the pressure of 62 kPa)

Figure 14 Working status of the soft gripper

Figure 15 shows the experimental results of grasping delicate objects of egg, strawberry, candy and knife. The successful grasping of egg and strawberry demonstrated the safety and adaptability of the webbed soft gripper for fragile and crisp objects, especially food and agricultural products. For the candy grasping experiment, 50 times grasping were executed for a pile of candies in a basket, as shown in Figure 15c. On average, there were 4 candies grabbed for each try, which can hardly be realized without the web. The packing effects of the web were also demonstrated by grasping the versatile knife without precise orientation or position, as shown in Figure 15d.

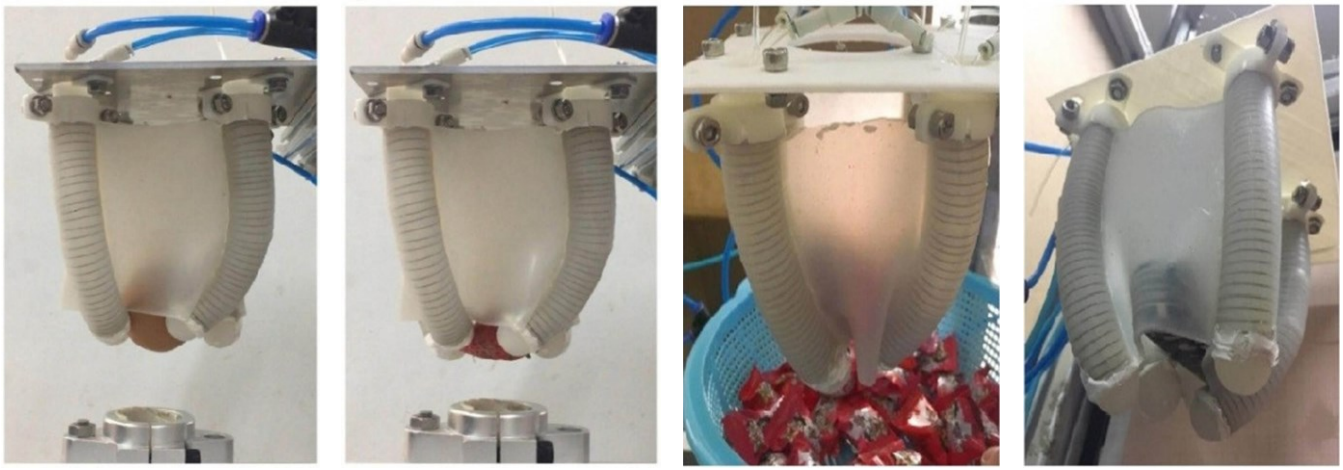

a. Grasping egg b. Grasping strawberry c. Grasping candies d. Grasping knife

Figure 15 Grasping experiments for different objects

4 Conclusions

Handling diverse fruits or food products is one of the grant challenges for harvesting robots and food equipment. Soft robotics provides a quite promising means to develop bio-inspired soft grippers to deal with this issue. In this study, a pneumatic webbed soft gripper was developed and evaluated. The mainly achieved conclusions are as follows:

1) The mechanical originality lies in the web structure design, which can effectively catch the scattered objects, prevent them from falling off the fingers, and reduce the precision requirements of modeling and control. The bionic structure greatly improves the stability and reliability of the grasping process.

2) The responses to the sinusoidal with the frequency of 0.2 Hz and 0.4 Hz and step excitation revealed that the developed multi-chambered finger has quite acceptable dynamic qualities of phase tracking and steady-state error.

3) The prototype of the soft gripper can grasp multiple objects at one grab, due to the webs around the fingers. This specific ability provides high practical possibility for aggregated fruits or food picking and placing.

Acknowledgements

This research was financially supported by the National Natural Science Foundation of China (Grant No. 51775499), the Key Research and Development Program of Zhejiang (Grand No. 2021C04015) and the Fundamental Research Funds for the Provincial Universities of Zhejiang (Grant No. RF-C2019004).

[References]

[1] Bao G J, Fang H, Chen L F, Wan Y H, Xu F, Zhang L B. Soft robotics: Academic insides and perspectives via bibliometric analysis. Soft Robotics, 2018; 5(3): 229–241.

[2] Lee C, Kim M, Kim Y J, Hong N, Ryu S, Kim H J. Soft robot review. International Journal of Control Automation and Systems, 2017; 15(1): 3–15.

[3] Paetsch W, Kaneko M. A three fingered, multijointed gripper for experimental use. In: Proceedings of the IEEE International Conference on Intelligent Robots and Systems, Ibaraki, Japan, 1990; 4077014. doi: 10.1109/IROS.1990.262505.

[4] Suzumori K, Iikura S, Tanaka H. Applying a flexible microactuator to robotic mechanisms. IEEE Control Systems, 1992; 12(1): 21–27.

[5] Jacobsen S C, Iversen E K, Knutti D F, Johnson R T. Design of the Utah/M.I.T. dextrous hand. In: Proceedings of the IEEE International Conference on Robotics and Automation, San Francisco, USA, 1986; pp.1520–1532.

[6] Xu T T, Yu J G, Vong C I, Wang B, Wu X Y, Zhang L. Dynamic morphology and swimming properties of rotating miniature swimmers with soft tails. IEEE/ASME Transactions on Mechatronics, 2019, 24(3): 924–934.

[7] Kumar K, Liu J, Christianson C, Ali M, Tolley M T, Aizenberg J. A biologically inspired, functionally graded end effector for soft robotics applications. Soft Robotics, 2017; 4(4): 317–323.

[8] Xu L, Chen H, Zou J, Dong W, Gu G, Zhu L. Bio-inspired annelid robot: A dielectric elastomer actuated soft robot. Bioinspiration and Biomimetics, 2017; 12(2): 025003. doi: 10.1088/1748-3190/aa50a5.

[9] Scholz M, Meyer J. Silicone rubber. Patent US9708458B2, USA, 2017.

[10] Sun Y, Song Y S, Paik J. Characterization of silicone rubber based soft pneumatic actuators. In: Proceedings of the 2013 IEEE/RSJ International Conference on Intelligent Robots and Systems, Tokyo, Japan, 2013; pp.4446–4453.

[11] Kern M D, Alcaide J O, Rentschler M E. Soft material adhesion characterization for in vivo locomotion of robotic capsule endoscopes: Experimental and modeling results. Journal of the Mechanical Behavior of Biomedical Materials, 2014; 39(1): 257–269.

[12] Yuan H, Yang J W, Zhang N W, Ren J. Tension properties of biodegradable PLA/Ecoflex blend film. Plastics, 2008; 37(6): 48–50.

[13] Schubert D W, Lämmlein M, Hanstein H V. Cyclic loading of model silicone elastomer samples with regard to the failure of silicone breast implants. Polymer Testing, 2018; 66(1): 292–295.

[14] Zhang Z, Ni X Q, Wu H L, Sun M, Bao G J, Wu H P, et al. Pneumatically actuated soft gripper with bistable structures. Soft Robotics, 2021; In press. doi: 10.1089/soro.2019.0195.

[15] Walker J, Zidek T, Harbel C, Yoon S, Strickland F S, Kumar S. Soft robotics: A review of recent developments of pneumatic soft actuators. Actuators, 2020; 9(1): 3. doi:10.3390/act9010003.

[16] Ogunmolu O P, Gu X J, Jiang S, Gans N R. Vision-based control of a soft robot for maskless head and neck cancer radiotherapy. In: Proceedings of the 2016 IEEE International Conference on Automation Science and Engineering (CASE), Fort Worth, USA, 2016; pp.256–262.

[17] Robertson M A, Sadeghi H, Florez J M, Paik J. Soft pneumatic actuator fascicles for high force and reliability. Soft Robotics, 2017; 4(1): 23–32.

[18] Laschi C, Cianchetti M, Mazzolai B, Margheri L, Follador M, Dario P. Soft robot arm inspired by the octopus. Advanced Robotics, 2012; 26(7): 709–727.

[19] Calderón A A, Ugalde J C, Zagal J C, Pérez-Arancibia N O. Design, fabrication and control of a multi-material-multi-actuator soft robot inspired by burrowing worms. In: Proceedings of the 2016 IEEE International Conference on Robotics and Biomimetics (ROBIO), Qingdao, China, 2016; pp.31–38.

[20] Caldwell D G, Medrano-Cerda G A, Goodwin M J. Braided pneumatic actuator control of a multi-jointed manipulator. In: Proceedings of the IEEE Systems Man and Cybernetics Conference, Le Touquet, France, 1993; pp.423–428.

[21] Martinez R V, Branch J L, Fish C R, Jin L H, Shepherd R F, Nunes R M D. Robotic tentacles with three-dimensional mobility based on flexible elastomers. Advanced Functional Materials, 2013; 25(2): 205–212.

[22] Tarvainen T V J, Yu W. Preliminary results on multi-pocket pneumatic elastomer actuators for human-robot interface in hand rehabilitation. In: Proceedings of the 2015 IEEE International Conference on Robotics and Biomimetics(ROBIO), Zhuhai, China, 2015; pp.2635–2639.

[23] Deimel R, Brock O. A compliant hand based on a novel pneumatic actuator. In: Proceedings of the IEEE International Conference on Robotics and Automation, Karlsruhe, Germany, 2013; pp.2047–2053.

[24] Taylor A J, Montayre R, Zhao Z, Kwok K W, Tse Z T H. Modular force approximating soft robotic pneumatic actuator. International Journal of Computer Assisted Radiology and Surgery, 2018; 13(11): 1819–1827.

[25] Martinez R V, Fish C R, Chen X, Whitesides G M. Elastomeric origami: Programmable paper‐elastomer composites as pneumatic actuators. Advanced Functional Materials, 2012; 22(7): 1376–1384.

[26] He M H, Song K, Mo H B, Li J, Pan D C, Liang Z Q. Progress on photosensitive resins for 3D printing. Journal of Functional Polymers, 2015; 28(1): 102–108.

[27] Yao P F, Gao T, Bao G J, Li K, Xu Z G, Wang Z H. Structure and bending model of long-arm biomimetic soft robot. Journal of Mechanical and Electrical Engineering, 2017; 34(4): 346–350.

[28] Wan W W, Harada K, Kanehiro F. Planning grasps with suction cups and parallel grippers using superimposed segmentation of object meshes. IEEE Transactions on Robotics, 2020; 99: 1–19.

[29] Yan L, Shen M, Yao W, Lu M Z, Liu L S, Xiao A L. Recognition method of lactating sows' posture based on sensor MPU6050. Transactions of the CSAM, 2015; 46(5): 279–285. (in Chinese)

[30] Wu X Y, Liu J, Huang C Y, Su M, Xu T T. 3-D path following of helical micro-swimmers with an adaptive orientation compensation model. IEEE Transactions on Automation Science and Engineering, 2020; 17(2): 823–832.